sGC stimulator praliciguat suppresses stellate cell fibrotic transformation and inhibits fibrosis and inflammation in models of NASH

Katherine C. Hall[a,b,1], Sylvie G. Bernier[a,b], Sarah Jacobson[a,b], Guang Liu[a,b], Ping Y. Zhang[a], Renee Sarno[a,b], Victoria Catanzano[a], Mark G. Currie[a,b], and Jaime L. Masferrer[a,b]

[a]Ironwood Pharmaceuticals, Cambridge, MA 02142; and [b]Cyclerion Therapeutics, Cambridge, MA 02142

Edited by Louis J. Ignarro, University of California, Los Angeles School of Medicine, Beverly Hills, CA, and approved April 10, 2019 (received for review December 11, 2018)

Endothelial dysfunction and reduced nitric oxide (NO) signaling are a key element of the pathophysiology of nonalcoholic steatohepatitis (NASH). Stimulators of soluble guanylate cyclase (sGC) enhance NO signaling; have been shown preclinically to reduce inflammation, fibrosis, and steatosis; and thus have been proposed as potential therapies for NASH and fibrotic liver diseases. Praliciguat, an oral sGC stimulator with extensive distribution to the liver, was used to explore the role of this signaling pathway in NASH. We found that sGC is expressed in hepatic stellate cells and stellate-derived myofibroblasts, but not in hepatocytes. Praliciguat acted directly on isolated hepatic stellate cells to inhibit fibrotic and inflammatory signaling potentially through regulation of AMPK and SMAD7. Using in vivo microdialysis, we demonstrated stimulation of the NO–sGC pathway by praliciguat in both healthy and fibrotic livers. In preclinical models of NASH, praliciguat treatment was associated with lower levels of liver fibrosis and lower expression of fibrotic and inflammatory biomarkers. Praliciguat treatment lowered hepatic steatosis and plasma cholesterol levels. The antiinflammatory and antifibrotic effects of praliciguat were recapitulated in human microtissues in vitro. These data provide a plausible cellular basis for the mechanism of action of sGC stimulators and suggest the potential therapeutic utility of praliciguat in the treatment of NASH.

praliciguat | soluble guanylate cyclase | NASH fibrosis | nitric oxide

Nonalcoholic fatty liver disease (NAFLD) is estimated to affect ∼30% of the population in the United States (1). Nonalcoholic steatohepatitis (NASH) is believed to develop when NAFLD leads to or is accompanied by inflammation that triggers the development of fibrosis. Steatosis and inflammation are both readily reversible and have little clinical impact; however, fibrosis regresses slowly and impairs liver function (2). Fibrotic tissue is generated when injury leads to the activation of hepatic stellate cells. These normally quiescent pericytes transdifferentiate into myofibroblasts that inappropriately secrete extracellular matrix (3). Thus, therapeutic strategies that interfere with fibrosis by targeting stellate cells and myofibroblasts are of great clinical interest (4).

Nitric oxide (NO) signals by binding and activating the intracellular receptor soluble guanylate cyclase (sGC) to catalyze the conversion of GTP to cGMP. sGC is a heterodimeric enzyme composed of an α and a β subunit that contains an NO-sensitive heme cofactor (5). Small molecule stimulators bind to and agonize sGC in the presence of the heme cofactor, thus enhancing NO signaling (6). Praliciguat, a novel sGC stimulator in clinical development, has pharmacokinetic properties consistent with once-a-day dosing and distributes extensively to the liver (7, 8).

Preclinically, sGC stimulators have improved cardiac parameters; decreased renal fibrosis; and suppressed inflammation, heart, and kidney dysfunction (7, 9). Antifibrotic and antiinflammatory effects have also been reported in models of liver fibrosis and portal hypertension (10–12).

In this study, the efficacy of the sGC stimulator praliciguat was tested in models of severe liver fibrosis and in a model incorporating metabolic perturbation with inflammation and fibrosis. Furthermore, the role of NO–sGC–cGMP signaling in the liver was elucidated through experiments that address the cellular location and regulation of sGC as well as the mechanism of action of sGC stimulators in fibrotic livers.

Results

sGC Is Expressed in Stellate Cells, but Not Hepatocytes. To identify cells that can respond to an sGC stimulator, tissue from normal rat livers was probed with antibodies against sGCα1 and sGCβ1 (Fig. 1*A*). Hepatocytes, the most common liver cell type, were negative for both subunits of sGC. However, stellate cells, with starlike morphology and containing lipid droplets, stained positive for both subunits of sGC. To confirm that stellate cells, but not hepatocytes, express sGC, isolated cultures of rat stellate cells and hepatocytes were treated with IWP-597 and DETA-NONOate (DETA), an NO donor. IWP-597 is an sGC stimulator with a potency similar to that of praliciguat (*SI Appendix*, Fig. S1). Stimulated stellate cells responded with robust generation of cGMP compared with

Significance

Nonalcoholic steatohepatitis (NASH) is an increasingly common disease characterized by liver steatosis and inflammation—with fibrosis being an important indicator of disease progression and severity—and is associated with reduced endothelial function and NO–soluble guanylate cyclase (sGC) signaling. Signaling downstream of NO can be restored using praliciguat, an sGC stimulator. Within the liver, stellate cells and myofibroblasts express sGC (unlike hepatocytes) and thus can be stimulated by praliciguat. Increased sGC activity inhibits fibrotic transformation and inflammatory responses in stellate cells potentially through AMPK and SMAD7. The effects on isolated stellate cells translate to human microtissues and in vivo models where treatment with praliciguat reduces inflammation, fibrosis, and steatosis. These preclinical results support further investigation of praliciguat as a potential therapy for NASH/fibrosis.

Author contributions: K.C.H., S.G.B., S.J., M.G.C., and J.L.M. designed research; K.C.H., S.G.B., S.J., G.L., P.Y.Z., R.S., and V.C. performed research; K.C.H., S.G.B., S.J., G.L., P.Y.Z., R.S., V.C., and J.L.M. analyzed data; and K.C.H. and J.L.M. wrote the paper.

Conflict of interest statement: All authors were employed by Ironwood Pharmaceuticals while conducting the research described in this manuscript. Authors may own Ironwood Pharmaceuticals stock or stock options.

This article is a PNAS Direct Submission.

[1]To whom correspondence should be addressed. Email: khall@cyclerion.com.

This article contains supporting information online at www.pnas.org/lookup/suppl/doi:10.1073/pnas.1821045116/-/DCSupplemental.

Published online May 13, 2019.

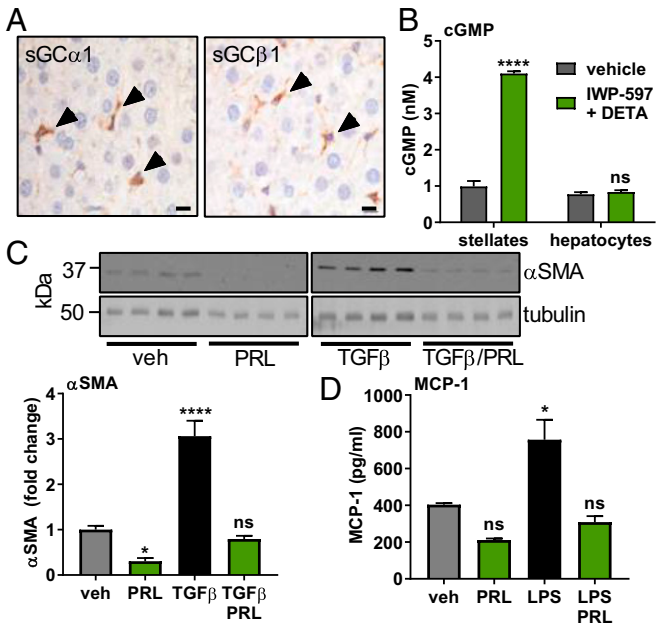

Fig. 1. Stimulation of sGC in stellate cells inhibits fibrotic and inflammatory signaling. (*A*) Rat liver sections stained with antibodies against sGCα1 and sGCβ1. Positive cells containing lipid droplets are indicated by arrowheads. (Scale bar: 10 μm.) (*B*) cGMP levels measured in rat stellate cells and hepatocytes after 30 min of stimulation with IWP-597 (0.1 μM) and DETA (30 μM). Unpaired *t* test. (*C*) Isolated rat stellate cells were cultured for 8 d, and the lysate was probed for α-SMA and tubulin. TGF-β (2.5 ng/mL) was added on the second day; praliciguat (PRL) (10 μM) on the fifth day. α-SMA signal was normalized to tubulin signal. Significance by one-way ANOVA and Dunnett's multiple comparison to vehicle. (*D*) Rat stellate cells cultured with praliciguat (10 μM) and/or LPS (0.1 μg/mL) for 24 h before MCP-1 levels were measured. ns, not significant; $*P \leq 0.05$; $****P \leq 0.0001$.

nonstimulated cells (Fig. 1*B*). In hepatocytes, basal cGMP levels were lower; 7.5× more cells were required to detect cGMP. Hepatocytes did not respond to stimulation (Fig. 1*B*). Similar results were obtained using human stellate cells and hepatocytes (*SI Appendix*, Fig. S2). Additionally, Kupffer cells (the resident macrophage in liver) and vascular smooth muscle cells express sGC and respond to stimulation, while endothelial cells exhibit a very low level of sGC activity (*SI Appendix*, Fig. S3 *A*, *B*, and *D*).

Praliciguat Suppresses Stellate Cell Response to TGF-β and Lipopolysaccharide. Isolated rat stellate cells were cultured with the profibrotic factor, TGF-β, to induce their transformation to alpha-smooth muscle actin (α-SMA)–expressing myofibroblasts. Praliciguat treatment completely prevented the TGF-β–induced increase in α-SMA protein (Fig. 1*C*).

Stellate cells were exposed to lipopolysaccharide (LPS) to activate an inflammatory response. Secretion of monocyte chemoattractant protein 1 (MCP-1), a key cytokine, was quantified. Incubation with LPS increased MCP-1 protein levels by 1.9-fold compared with control cells. Coincubation with praliciguat completely prevented the LPS-induced increase in MCP-1 (Fig. 1*D*). Stimulation of Kupffer cells with LPS resulted in secretion of IL-1β and TNF-α. No effect of treatment with IWP-597 was observed (*SI Appendix*, Fig. S3*C*).

Myofibroblasts in Fibrotic Tissue Express sGC. Having confirmed that stellate cells in healthy livers express sGC, expression was assessed in fibrotic liver tissue. Fibrotic bridges stained positive for both the α and β subunits of sGC, suggesting that stellate-derived myofibroblasts express sGC. Hepatocytes in fibrotic livers were negative for staining of both subunits (Fig. 2*A*). To quantitate levels of sGC in normal and fibrotic tissues, the expression level of sGC genes was measured. Expression of the gene for sGCα1 (*Gucy1A1*) was greater by 2.5-fold, and expression of the gene for sGCβ1 (*Gucy1B1*) was greater by 1.9-fold in tissue from fibrotic livers compared with healthy livers (Fig. 2*B*). Gene expression of the downstream NO–sGC–cGMP pathway members—protein kinase G (PKG) and vasodilator-stimulated phosphoprotein (VASP)—was also higher in fibrotic tissue than in normal tissue. Similar changes in gene expression were also measured in other models (*SI Appendix*, Fig. S4). Fibrotic livers contained a greater amount of both sGCβ1/GAPDH protein (3.9 ± 0.1 vs. 2.7 ± 0.4 a.u., $P < 0.05$; 1.4-fold increase) and α-SMA/GAPDH protein (4.5 ± 1.1 vs. 0.8 ± 0.1 a.u., $P < 0.01$; sixfold increase) than livers from animals given vehicle (Fig. 2*C*).

To directly determine the activation of sGC in vivo, microdialysis was used to measure cGMP. In normal livers, basal levels of cGMP were 1.0 ± 0.5 nM. Addition of sodium nitroprusside (SNP), an NO donor, increased cGMP levels to 3.2 ± 1.4 nM. Addition of praliciguat resulted in cGMP levels of 5.5 ± 0.9 nM. cGMP levels reached 19.2 ± 1.6 nM upon simultaneous addition of praliciguat and SNP.

cGMP levels were similar in fibrotic and control liver tissues (1.1 ± 0.1 vs. 0.8 ± 0.1 nM) (Fig. 2*D*). After treatment with praliciguat, the cGMP level in fibrotic livers was greater than that in normal livers (12× baseline vs. 6× baseline). Furthermore, perfusion with a mixture of SNP and praliciguat induced a 60-fold increase in cGMP level in carbon tetrachloride (CCl_4)-treated fibrotic livers compared with a 20-fold increase in normal livers (Fig. 2*D*).

Orally dosing normal rats with praliciguat resulted in higher levels of cGMP in the liver dialysate as compared with vehicle-treated rats (1.9 ± 0.3 nM vs. 0.9 ± 0.9 nM, respectively, Fig. 2*E*).

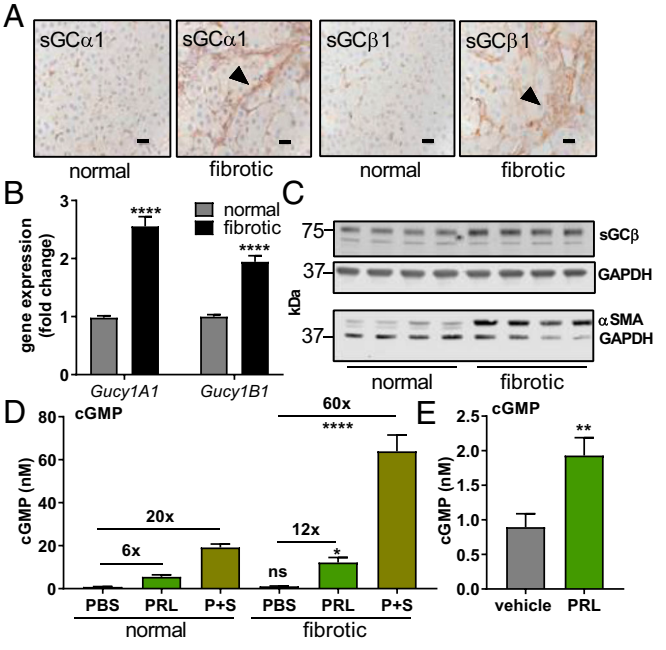

Fig. 2. sGC and cGMP in normal and fibrotic livers. (*A*) Sections of livers from vehicle (normal) and CCl_4 (fibrotic) groups were stained with antibodies against sGCα1 and sGCβ1. Arrowheads denote fibrotic bridges. (Scale bar: 25 μm.) (*B*) mRNA levels for the sGCα1 and sGCβ1 genes. (*C*) Western blots for sGCβ1, α-SMA, and GAPDH were performed on liver lysate. (*D*) cGMP production in response to stimulation was measured in the control group ($n = 8$) and the CCl_4-induced fibrosis group ($n = 7$). PBS (vehicle), praliciguat (PRL) (1 mg/mL), and SNP (S) (100 μM) plus praliciguat (1 mg/mL) were locally delivered by retrodialysis. (*E*) Levels of cGMP in the liver after 4 d of oral dosing with praliciguat (10 mg/kg) ($n = 15$) or vehicle ($n = 10$). Significance determined using an unpaired *t* test. ns, not significant; $*P \leq 0.05$; $**P \leq 0.01$; $****P \leq 0.0001$.

Praliciguat Reduces Fibrosis and Inflammation in CCl_4-Induced Fibrosis. CCl_4 treatment induced extensive bridging fibrosis: 14% of the tissue area was positive for collagen compared with less than 1% positive area in the vehicle group as assessed by picrosirius red (PSR) staining. Praliciguat treatment had the greatest effect when dosed at 3 mg/kg per day; collagen-positive area was 33% less than in the CCl_4 control group (Fig. 3*A*). Nineteen percent of tissue was positive for α-SMA. In the groups treated with 1, 3, and 10 mg/kg per day of praliciguat, α-SMA–positive tissue area was respectively 20%, 29%, and 21% less than in the CCl_4 control group (Fig. 3*B*). Hepatic hydroxyproline content was decreased in the 1 and 3 mg/kg per day groups, reaching statistical significance in the 10 mg/kg per day group (Fig. 3*C*). Similar effects of praliciguat on PSR and α-SMA staining were observed in the thioacetamide (TAA) model (*SI Appendix*, Fig. S5 *A* and *B*).

Hepatic expression of genes encoding the fibrotic markers TGF-β (*Tgfb*), PDGF-β (*Pdgfb*), α-SMA (*Acta2*), and MMP2 (*Mmp2*) were up-regulated in the liver tissue of animals in the CCl_4 control group. Treatment with 1, 3, and 10 mg/kg per day of praliciguat suppressed the increase in TGF-β and PDGF-β gene expression. Expression of the genes for *Mmp2* and α-SMA were lower in the 3 and 10 mg/kg per day praliciguat groups than in the CCl_4 group (Fig. 3*D* and *SI Appendix*, Fig. S5*C*).

Levels of phosphorylated AMPK (pAMPK) (Ser-108) and SMAD7 were significantly lower in the CCl_4 control group liver samples compared with the vehicle group. In the group that received 3 mg/kg per day of praliciguat, levels of pAMPK and SMAD7 were significantly greater than those in the CCl_4 control group (Fig. 3*E*).

Liver enzymes—alanine aminotransferase (ALT) and aspartate transaminase (AST)—were elevated in the CCl_4 group, indicating hepatic damage, and were comparatively lower in all three treatment groups (Fig. 4*A*). To assess the level of macrophage infiltration in the CCl_4 model, liver sections were stained for the macrophage marker CD68. In the vehicle control group, 2% of the tissue area stained positive. In rats treated with CCl_4, 14% of the liver stained positive for macrophages; however, in the 3 mg/kg per day praliciguat group, only 10% of the total tissue was positive, indicating reduced levels of infiltrating macrophages (Fig. 4*B*).

Hepatic expression of genes for the inflammatory markers TNF-α (*Tnfa*) and MCP-1 (*Ccl2*) was up-regulated in the CCl_4 model. MCP-1 gene expression was lower in rats treated with 1, 3, and 10 mg/kg per day of praliciguat than in the CCl_4 group. TNF-α gene expression was lower in the 3 and 10 mg/kg per day praliciguat groups than in the CCl_4 control group (Fig. 4*C*). Plasma TNF-α levels were found to be significantly greater in the CCl_4 group than in the control group. TNF-α levels were normalized in both 1 and 3 mg/kg per day praliciguat groups (*SI Appendix*, Fig. S5*D*).

Greater amounts of NF-κB p65 was observed in the CCl_4 control group than in the vehicle group. The amount of p65 was significantly decreased in the group that received 3 mg/kg per day of praliciguat compared with the CCl_4 control group (Fig. 4*D*).

Praliciguat Ameliorated Liver Damage in the STAM/HC Model. In the steatosis and metabolism with high cholesterol (STAM/HC) mouse model of NASH, ALT and AST levels were respectively twofold and threefold higher compared with the control group. Enzyme levels in the groups treated with 3 and 10 mg/kg per day of praliciguat were similar to vehicle animals (Fig. 5*A*). Compared with the vehicle group, plasma cholesterol was elevated in the STAM/HC group. This increase in plasma cholesterol was attenuated by 21% in both treatment groups (Fig. 5*B*). The increase in liver triglycerides observed in the STAM/HC control group was reduced by 25% in the 10 mg/kg per day praliciguat group (Fig. 5*C*). Additionally, levels of hydroxyproline and expression of fibrotic and inflammatory genes were increased in the STAM/HC control group but were comparatively lower in the praliciguat-treated groups (*SI Appendix*, Fig. S6).

sGC Expression and Activity in Human 3D Cell Culture Model. cGMP was below the level of detection in untreated microtissues composed of hepatocytes, Kupffer, stellate, and liver sinusoidal endothelial cells. Stimulation with IWP-597 and DETA induced robust production of cGMP (3.95 ± 0.21 nM) (Fig. 6*A*). In histological sections of microtissues cultured with TGF-β for 7 d, α-SMA was detected around the periphery of the microsphere (Fig. 6*B*). TGF-β treatment of microtissues increased expression of the gene encoding α-SMA (*Acta2*) by 1.5-fold, indicating the induction of fibrosis. Incubation with the sGC stimulator blunted the response to TGF-β (Fig. 6*C*). Microtissues treated with IWP-597 and DETA in addition to TGF-β secreted 39% less MCP-1 protein than those incubated with TGF-β alone (Fig. 6*D*).

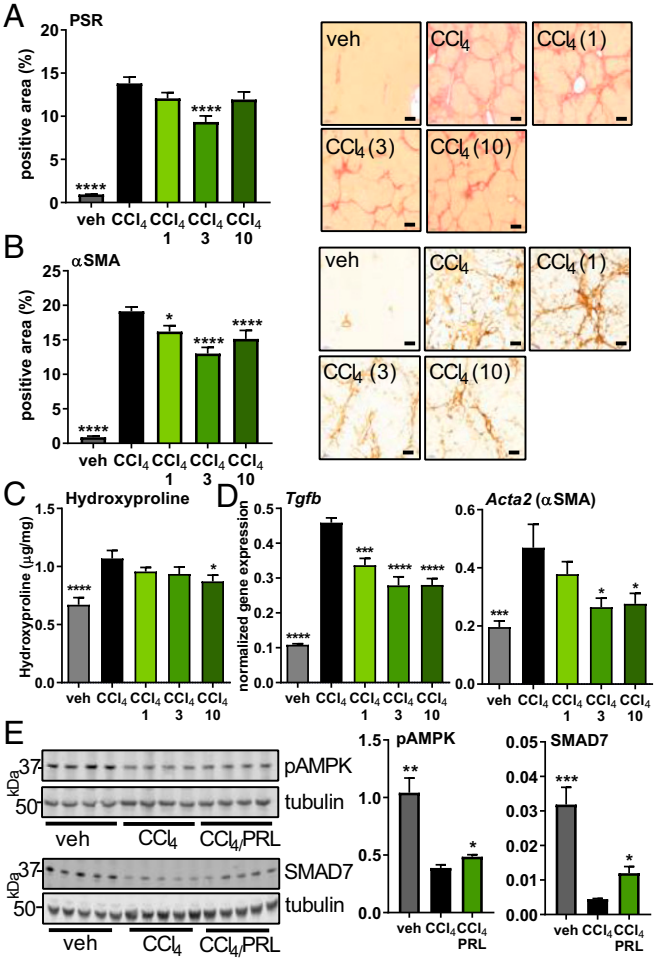

Fig. 3. Antifibrotic effect of praliciguat in the CCl_4 model. Experimental groups are vehicle (corn oil) ($n = 12$), CCl_4 alone ($n = 12$), or CCl_4 with 1 ($n = 12$), 3 ($n = 12$), or 10 mg/kg ($n = 12$) of praliciguat per day. (*A*, *Left*) PSR-positive tissue area. Data analyzed by one-way ANOVA followed by Fisher's least significant difference comparison with the CCl_4 group. (*A*, *Right*) Representative images of a tissue section from each group. (Scale bar: 200 μm.) (*B*, *Left*) Quantification of α-SMA–positive tissue area for each experimental group. (*B*, *Right*) Representative images of a tissue section from each group. (Scale bar: 100 μm.) (*C*) Hepatic hydroxyproline content in each experimental group. (*D*) mRNA expression levels of fibrotic markers in liver tissue: *Tgfb* and *Acta2*. Data analyzed using one-way ANOVA followed by Dunnett's multiple comparison with the CCl_4 group alone. (*E*) Liver lysate from vehicle, the CCl_4 control group, and the 3 mg/kg per day praliciguat (PRL) group were probed for pAMPK (Ser-108), SMAD7, and tubulin. Unpaired *t* tests comparing each condition to the CCl_4-alone group. $^*P \le 0.05$, $^{**}P \le 0.01$, $^{***}P \le 0.001$, $^{****}P \le 0.0001$.

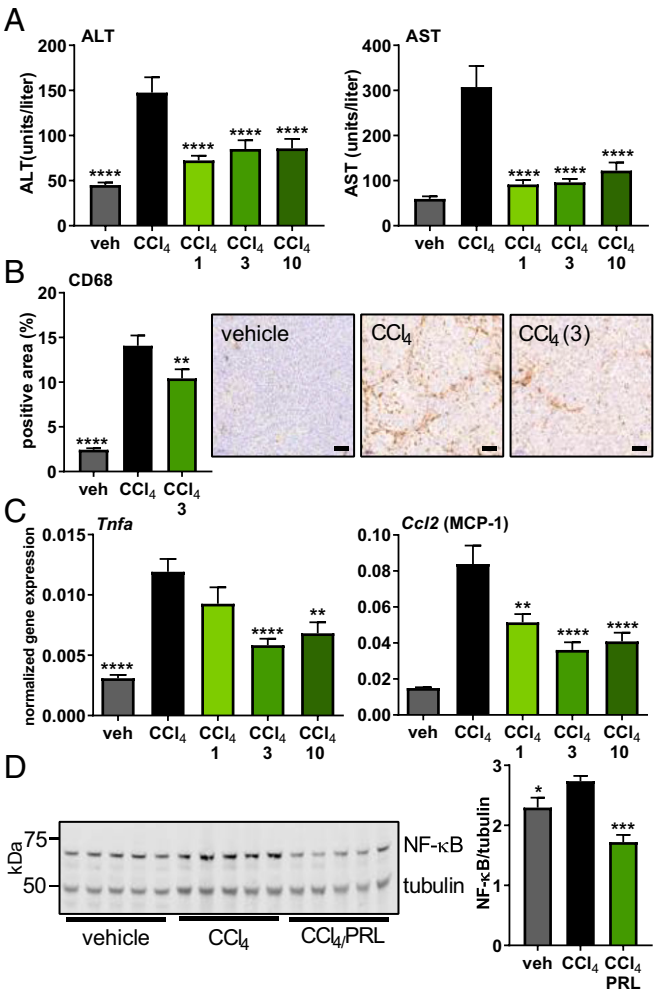

Fig. 4. Reduction of local and systemic inflammation in praliciguat-treated groups in the CCl_4 model. (*A*) ALT and AST liver-enzyme plasma levels were quantified in samples from all groups. Significance determined using one-way ANOVA followed by Dunnett's multiple comparison with the CCl_4 group. (*B*, *Left*) Quantification of area staining positive for the macrophage marker CD68 from vehicle, the CCl_4 group, and the praliciguat (3 mg/kg per day) group. Data analyzed by one-way ANOVA followed by Fisher's least significant difference comparison with the CCl_4 group. (*B*, *Right*) Representative images of a stained tissue section from each group. (Scale bar: 100 μm.) (*C*) mRNA expression levels in liver tissue of the inflammation markers Tnfa and *Ccl2*. (*D*) Liver lysate from vehicle, the CCl_4 control group, and the 3 mg/kg per day praliciguat (PRL) group were probed for p65 and tubulin. Signal for p65 was normalized to tubulin signal and presented as a ratio. Unpaired *t* tests comparing each condition to the CCl_4-alone group. $*P \leq 0.05$, $**P \leq 0.01$, $***P \leq 0.001$, and $****P \leq 0.0001$.

however, levels in praliciguat-treated cells were significantly higher, although not restored to vehicle levels (Fig. 6*E*).

Location of sGCβ in Human Tissue. Human histological liver sections ($n = 4$) were obtained from patients diagnosed as normal or as having NASH/fibrosis. In normal liver samples, sGCβ1 was detected in perisinusoidal cells whose location and shape were consistent with that of stellate cells. Similar to the observations made in rat tissue, no staining was detected in human hepatocytes (Fig. 6*F*). Within the diseased samples, there were nonfibrotic regions where sGCβ1 localization resembled healthy tissue. However, within the fibrotic bridges that stained heavily positive for α-SMA, multiple sGCβ1-positive clusters of fibroblast-like cells were observed (Metavir stage F3, Fig. 6*G*). Furthermore, sGCβ1 was detected around hepatic blood vessels.

Discussion

We present unequivocal evidence that sGC is expressed and active in stellate and Kupffer cells, but not in hepatocytes. This finding contrasts with other studies that report sGC expression in hepatocytes (12, 13). In our study, we measured sGC activity in isolated hepatocytes and found that rat and human hepatocytes cannot be stimulated to produce cGMP with an NO donor, with praliciguat, or with a combination. In contrast, isolated primary stellate cells clearly responded to sGC stimulation. Stellate cell expression of sGC was further demonstrated using immunohistochemistry with specific antibodies against sGCα1 and sGCβ1. Again, hepatocytes had no positive signal. Furthermore, the immunohistochemical staining of fibrotic tissues provides evidence that stellate cell sGC expression is maintained after their activation to myofibroblasts. Given the central role of stellate cells in liver fibrosis (14), therapeutic approaches that specifically target stellate cells and stellate cell-derived myofibroblasts in NASH are expected to have great impact on the disease (4).

A key feature of sGC signaling in fibrotic stellate cells was unraveled using in vivo microdialysis to pharmacologically study sGC activation in normal liver and in the CCl_4 fibrosis model. While total sGC mRNA and protein was increased in fibrotic livers, the enzymatic activity was not increased. This apparent disconnect is most likely due to the low availability of NO due to depletion by reactive oxygen species (15) or dysregulation of endothelial NOS (16, 17). After praliciguat stimulation, a greater amount of cGMP was generated by fibrotic livers compared with normal livers, consistent with the presence of unstimulated sGC. We hypothesize that this sGC activity accounts for the positive pharmacological effects observed here in multiple models of liver disease. sGC stimulators are uniquely suited to restoring cGMP-dependent signaling in a low-NO state due to their ability to synergize with NO to activate sGC as previously demonstrated in HEK cells (7) and illustrated here in vivo using microdialysis.

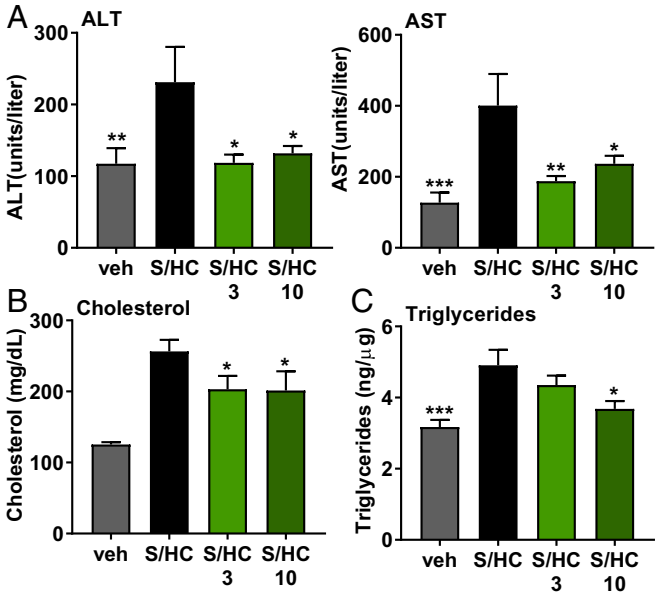

Fig. 5. Praliciguat treatment attenuates inflammation and steatosis in the STAM/HC model of NASH. Experimental groups are vehicle ($n = 9$), STAM/HC (S/HC) ($n = 7$), STAM/HC with 3 mg/kg per day of praliciguat ($n = 9$), and STAM/HC with 10 mg/kg per day of praliciguat ($n = 7$). (*A*) ALT and AST plasma levels. Data analyzed using one-way ANOVA followed by Fisher's least significant difference test comparing all other groups to the STAM/HC group. (*B*) Cholesterol was measured in plasma. Data presented in micrograms of cholesterol per deciliter of plasma. (*C*) Triglyceride levels in the liver are expressed as nanograms of triglycerides per microgram of protein.

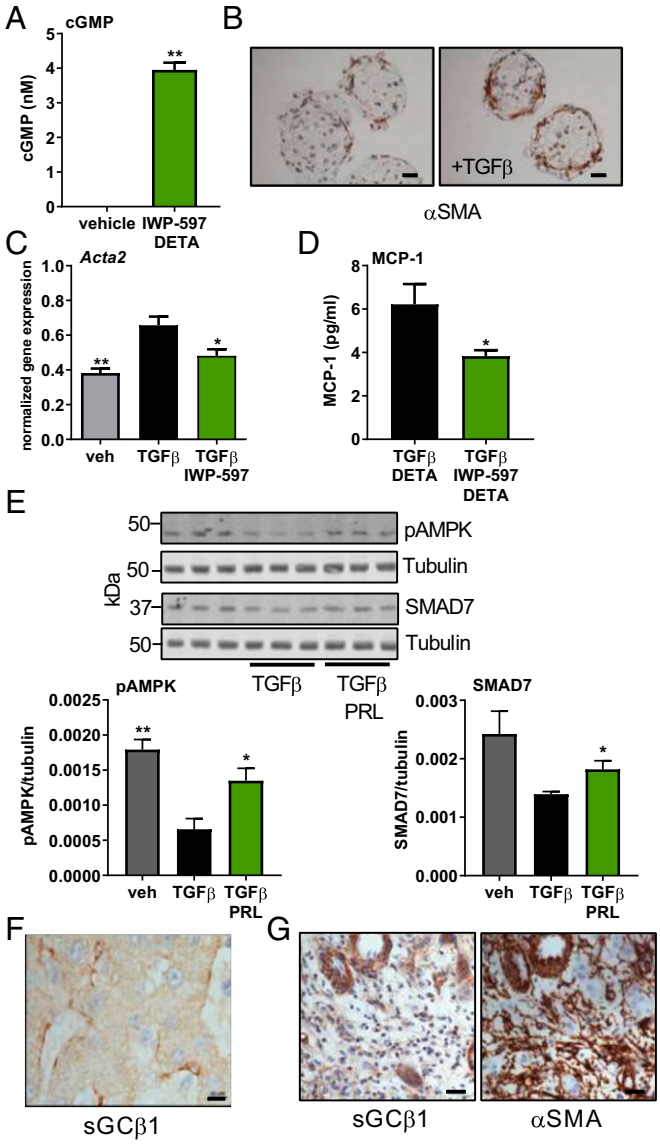

Fig. 6. sGC in human tissues. (*A*) Human liver microtissue cultures were stimulated with IWP-597 (10 μM) and DETA (30 μM) ($n = 2$) for 30 min. cGMP levels in the vehicle-treated cultures were below detection levels. Data analyzed using an unpaired *t* test. (*B*) Sections of microtissues incubated in control or TGF-β–containing media were stained for α-SMA. (Scale bar: 25 μm.) (*C*) The gene expression levels for *Acta2* were measured in microtissues treated with TGF-β (3 ng/mL) and IWP-597 (10 μM) for 48 h. Data analyzed by one-way ANOVA followed by Dunnett's multiple comparison with TGF-β alone. (*D*) MCP-1 protein was measured in the cell media of microtissues treated with TGF-β and DETA ($n = 7$) or with TGF-β, IWP-597, and DETA ($n = 6$) for 48 h. Unpaired *t* test. (*E*, *Upper*) Human stellate cells cocultured with hepatocytes were treated with TGF-β (2.5 ng/mL) with or without praliciguat (PRL) (10 μM) and DETA- (10 μM) for 5 d, and lysate was probed for pAMPK (Ser-108), SMAD7, and tubulin. (*E*, *Lower*) pAMPK and SMAD7 signals were normalized to tubulin signal and are presented as a ratio. Unpaired *t* tests comparing each condition to TGF-β alone. (*F*) Formalin-fixed, paraffin-embedded healthy human liver stained for sGCβ1. (Scale bar: 10 μm.) (*G*) Serial sections fibrotic human liver stained for sGCβ1 and α-SMA. (Scale bar: 25 μm.) $*P \leq 0.05$, $**P \leq 0.01$.

Praliciguat displayed robust antifibrotic effects in cell culture assays and animal models. Praliciguat suppressed TGF-β–induced stellate cell activation, demonstrating that sGC stimulation is antifibrotic in rat and human stellate cells. This effect may be general to prefibrotic cell types because modulation of the NO–sGC–cGMP pathway has been found to inhibit fibroblast-to-myofibroblast transformation in lung fibroblasts and dermal fibroblasts (18–20). Consistent with the in vitro results, in vivo expression of TGF-β target genes, such as *Acta2* and *Mmp2*, was attenuated in praliciguat-treated groups. In addition, praliciguat-treated groups expressed lower levels of TGF-β and PDGF-β, considered master drivers of fibrosis, compared with nontreated groups.

Interestingly, praliciguat did not modulate the canonical TGF-β signaling pathway in stellate cells as assessed by phosphorylated SMAD2 and SMAD3. However, in vitro and in vivo praliciguat treatment resulted in increased levels of SMAD7, a pathway member known to antagonize TGF-β signaling (21, 22). Additionally, levels of the activated pAMPK (Ser-108) followed a similar pattern. AMPK activation has been reported to increase SMAD7 (23). We propose a model in which active PKG, resulting from sGC stimulation and cGMP signaling, leads to AMPK phosphorylation and SMAD7 up-regulation, resulting in inhibition of profibrotic TGF-β signaling (*SI Appendix*, Fig. S7). This molecular mechanism could explain the observed antifibrotic activity of praliciguat.

The observations that praliciguat's effect on some end points appears to be less effective at the highest dose may be due to unexpectedly high plasma levels of compound in the 10 mg/kg per day group. The doses used were selected based the general pharmacological effects observed with praliciguat (7). The lower doses of praliciguat (1 and 3 mg/kg per day) resulted in plasma levels consistent with little or no effect on blood pressure (<5 to 10 mmHg). However, the 10 mg/kg per day dose resulted in plasma exposures that would reduce mean arterial blood pressure by ∼15 to 20 mmHg. This reduction in mean arterial pressure could activate the renin–angiotensin system, a phenomenon that been associated with pathology of liver diseases (24). Thus, it may partially oppose the antiinflammatory and antifibrotic effects of praliciguat. Clinical doses of praliciguat resulted in exposures similar to those observed in groups receiving 1 and 3 mg/kg per day (25).

Praliciguat's suppression of LPS induction of MCP-1 secretion reveals that sGC stimulation can directly inhibit the up-regulation of an inflammatory signaling molecule in stellate cells. Consistent with praliciguat's in vitro effect, hepatic expression of *Ccl2*, the gene for MCP-1, was lower in the praliciguat-treated groups of the CCl_4 and STAM/HC models. MCP-1 has been shown to mediate macrophage/monocyte infiltration into the liver (26, 27), and the lower expression of *Ccl2* may explain the observed decrease in hepatic macrophage infiltration. On a molecular level, praliciguat treatment resulted in comparatively less of the NF-κB subunit p65, potentially due to SMAD7-mediated down-regulation (28) as schematized in *SI Appendix*, Fig. S7. While many of praliciguat antiinflammatory effects could be mediated by stellate cells, praliciguat may also impact the inflammatory cells involved in liver fibrosis, such as Kupffer cells and infiltrating macrophages or neutrophils (29). Elucidation of the effect of sGC stimulation on Kupffer and other inflammatory cells during fibrogenesis requires further investigation.

To investigate the role of sGC in metabolically driven liver fibrosis, we studied the STAM/HC model, in which insulin deficiency is combined with a high-fat, high-cholesterol diet to induce hepatic inflammation and fibrosis. Praliciguat-treated groups exhibited lower levels of inflammatory and fibrotic markers. In addition, praliciguat treatment decreased levels of plasma cholesterol and hepatic triglycerides, which is consistent with observations made in a diet-induced obesity (DIO) mouse model in which hepatic steatosis and levels of hepatic triglycerides were attenuated by praliciguat (11). Similar effects in the DIO model were previously noted with a different sGC stimulator, Bay 41-8543 (30). In an exploratory phase 2 clinical study, subjects with type 2 diabetes and controlled hypertension who received daily praliciguat for 2 wk had lower levels of plasma LDL cholesterol and triglycerides than the subjects receiving placebo, suggesting that praliciguat can also affect metabolism in humans (25). Although, further studies will be needed to clarify the exact mechanism behind this metabolic modulation; our current findings suggest a role for AMPK, a pathway recently suggested to be the connection between nitrate–nitrite–NO signaling and decreased steatosis (31).

In conclusion, we have shown that hepatic stellate cells and myofibroblasts are the main hepatic cell types that respond to praliciguat, while hepatocytes do not. Moreover, sGC stimulation of rat stellate cells as well as human liver microtissues inhibited TGF-β–induced fibrotic biomarker expression and MCP-1 secretion, identifying a mechanism by which sGC stimulation exerts an antiinflammatory effect. In vivo, praliciguat and NO acted synergistically to stimulate cGMP production by sGC. In fibrotic livers, increased sGC expression is likely due to the greater number of myofibroblasts compared with the number of stellate cells in healthy livers. The antifibrotic effects of sGC stimulation observed in vitro correlate with fewer myofibroblasts, less collagen deposition, and lowers levels of fibrotic biomarkers in the CCl_4, TAA, and STAM/HC models of liver fibrosis. Antiinflammatory effects were observed in the CCl_4 and STAM/HC models, in which decreased hepatic macrophage infiltration, plasma TNF-α, and biomarkers of inflammation were noted in praliciguat-treated groups. Finally, in the STAM/HC model, praliciguat-treated groups had lower levels of hepatic triglycerides and plasma cholesterol compared with vehicle-treated groups. These preclinical data illustrate the multidimensional pharmacology of praliciguat and support further examination of its therapeutic use in NASH, a disease characterized by hepatic steatosis, inflammation, and fibrosis.

Materials and Methods

Compounds and Chemicals. Praliciguat and IWP-597 were synthesized at Ironwood Pharmaceuticals. Other chemicals were purchased from Sigma-Aldrich, unless otherwise noted.

Animal Models. All animal-use protocols were reviewed and approved by the Institutional Animal Care and Use Committee of Ironwood Pharmaceuticals. The STAM/HC model was performed as described in Fujii et al. (32) with the modification that 2% cholesterol was added to the high-fat diet. Praliciguat treatment began at 6 wk of age and continued until study end at 12 wk of age.

For CCl_4 fibrosis induction with praliciguat treatment, CCl_4 was administered for 8 wk. Praliciguat treatment commenced 2 wk after the study began. For CCl_4 fibrosis induction and microdialysis, CCl_4 was administered for 4 wk before microdialysis. For microdialysis, a linear microdialysis probe (BASi) was inserted into the right medial lobe of the liver and perfused with PBS, SNP (100 μM), or praliciguat (1 mg/mL) at a rate of 2.5 μL/min for 60 min. Dialysate cGMP levels were quantified using an enzyme immunoassay for cGMP according to the acetylation protocol provided by the manufacturer (GE Amersham). Analysis of liver and plasma samples is described in the *SI Appendix, Supplemental Materials and Methods*.

Hepatocyte and Stellate Cell Culture and Human Liver Microtissues. Human primary hepatic stellate cells (ZenBio), human primary hepatocytes, cryopreserved rat primary hepatic stellate cells, and hepatocytes (In Vitro ADMET Laboratories) were cultured according to standard practices and as described in *SI Appendix, Supplemental Materials and Methods*. Human microtissues were purchased from InSphero and cultured according to the manufacturer's instructions with modifications as described in *SI Appendix, Supplemental Materials and Methods*.

sGC Enzyme Assay and sGC Whole-Cell Assay. These assays were conducted as previously described (7).

RNA Expression Levels. Gene expression in the tissue homogenates was measured using a QuantiGene 2.0 Plex Assay (Affymetrix/Life Technologies) following the user's manual. Analytes were measured using Luminex MAGPIX (Bio-Rad). Signal was normalized to housekeeping genes.

Western Blotting. Western blotting was performed using standard methods and the antibodies described in *SI Appendix, Supplemental Materials and Methods*. Expression of the protein of interest was normalized to the expression of a housekeeping protein (tubulin or GAPDH), and data are presented as a ratio or as fold change over a baseline condition where noted.

Statistics. Results were analyzed by the statistical test described in the figure legends using GraphPad Prism v7.02 software (GraphPad Software, Inc.), with P values of >0.05 not significant and $^{*}P \leq 0.05$, $^{**}P \leq 0.01$, $^{***}P \leq 0.001$, and $^{****}P \leq 0.0001$.

ACKNOWLEDGMENTS. We thank Todd Milne, Albert Profy, and Jennifer Chickering for their careful reading of this work and their helpful suggestions.

1. Browning JD, et al. (2004) Prevalence of hepatic steatosis in an urban population in the United States: Impact of ethnicity. *Hepatology* 40:1387–1395.
2. Diehl AM, Day C (2017) Cause, pathogenesis, and treatment of nonalcoholic steatohepatitis. *N Engl J Med* 377:2063–2072.
3. Hernandez-Gea V, Friedman SL (2011) Pathogenesis of liver fibrosis. *Annu Rev Pathol* 6:425–456.
4. Higashi T, Friedman SL, Hoshida Y (2017) Hepatic stellate cells as key target in liver fibrosis. *Adv Drug Deliv Rev* 121:27–42.
5. Derbyshire ER, Marletta MA (2012) Structure and regulation of soluble guanylate cyclase. *Annu Rev Biochem* 81:533–559.
6. Evgenov OV, et al. (2006) NO-independent stimulators and activators of soluble guanylate cyclase: Discovery and therapeutic potential. *Nat Rev Drug Discov* 5:755–768.
7. Tobin JV, et al. (2018) Pharmacological characterization of IW-1973, a novel soluble guanylate cyclase stimulator with extensive tissue distribution, antihypertensive, anti-inflammatory, and antifibrotic effects in preclinical models of disease. *J Pharmacol Exp Ther* 365:664–675.
8. Buys ES, et al. (2018) Discovery and development of next generation sGC stimulators with diverse multidimensional pharmacology and broad therapeutic potential. *Nitric Oxide* 78:72–80.
9. Geschka S, et al. (2011) Soluble guanylate cyclase stimulation prevents fibrotic tissue remodeling and improves survival in salt-sensitive Dahl rats. *PLoS One* 6:e21853.
10. Knorr A, et al. (2008) Nitric oxide-independent activation of soluble guanylate cyclase by BAY 60-2770 in experimental liver fibrosis. *Arzneimittelforschung* 58:71–80.
11. Flores-Costa R, et al. (2018) The soluble guanylate cyclase stimulator IW-1973 prevents inflammation and fibrosis in experimental non-alcoholic steatohepatitis. *Br J Pharmacol* 175:953–967.
12. Schwabl P, et al. (2018) The soluble guanylate cyclase stimulator riociguat reduces fibrogenesis and portal pressure in cirrhotic rats. *Sci Rep* 8:9372.
13. Minin EA, et al. (2005) L-Arginine-NO-cGMP signaling following acute liver injury in the rat. *Exp Toxicol Pathol* 57:161–171.
14. Mederacke I, et al. (2013) Fate tracing reveals hepatic stellate cells as dominant contributors to liver fibrosis independent of its aetiology. *Nat Commun* 4:2823.
15. Sánchez-Valle V, Chávez-Tapia NC, Uribe M, Méndez-Sánchez N (2012) Role of oxidative stress and molecular changes in liver fibrosis: A review. *Curr Med Chem* 19:4850–4860.
16. Rockey DC, Chung JJ (1998) Reduced nitric oxide production by endothelial cells in cirrhotic rat liver: Endothelial dysfunction in portal hypertension. *Gastroenterology* 114:344–351.
17. Persico M, et al. (2017) "Non alcoholic fatty liver disease and eNOS dysfunction in humans". *BMC Gastroenterol* 17:35.
18. Beyer C, et al. (2015) Stimulation of the soluble guanylate cyclase (sGC) inhibits fibrosis by blocking non-canonical TGFβ signalling. *Ann Rheum Dis* 74:1408–1416.
19. Zenzmaier C, et al. (2015) Activators and stimulators of soluble guanylate cyclase counteract myofibroblast differentiation of prostatic and dermal stromal cells. *Exp Cell Res* 338:162–169.
20. Dunkern TR, Feurstein D, Rossi GA, Sabatini F, Hatzelmann A (2007) Inhibition of TGF-beta induced lung fibroblast to myofibroblast conversion by phosphodiesterase inhibiting drugs and activators of soluble guanylyl cyclase. *Eur J Pharmacol* 572:12–22.
21. Hayashi H, et al. (1997) The MAD-related protein Smad7 associates with the TGFbeta receptor and functions as an antagonist of TGFbeta signaling. *Cell* 89:1165–1173.
22. Nakao A, et al. (1997) Identification of Smad7, a TGFbeta-inducible antagonist of TGF-beta signalling. *Nature* 389:631–635.
23. Stone JD, Holt AW, Vuncannon JR, Brault JJ, Tulis DA (2015) AMP-activated protein kinase inhibits transforming growth factor-β-mediated vascular smooth muscle cell growth: Implications for a Smad-3-dependent mechanism. *Am J Physiol Heart Circ Physiol* 309:H1251–H1259.
24. Simões E Silva AC, Miranda AS, Rocha NP, Teixeira AL (2017) Renin angiotensin system in liver diseases: Friend or foe? *World J Gastroenterol* 23:3396–3406.
25. Hanrahan, JP, et al. (2018) Fourteen-day study of praliciguat, a soluble guanylate cyclase stimulator, in patients with diabetes and hypertension. *Diabetes* 67(Suppl 1):74.
26. Miura K, Yang L, van Rooijen N, Ohnishi H, Seki E (2012) Hepatic recruitment of macrophages promotes nonalcoholic steatohepatitis through CCR2. *Am J Physiol Gastrointest Liver Physiol* 302:G1310–G1321.
27. Marra F, et al. (1998) Increased expression of monocyte chemotactic protein-1 during active hepatic fibrogenesis: Correlation with monocyte infiltration. *Am J Pathol* 152:423–430.
28. Wang W, et al. (2005) Signaling mechanism of TGF-beta1 in prevention of renal inflammation: Role of Smad7. *J Am Soc Nephrol* 16:1371–1383.
29. Koyama Y, Brenner DA (2017) Liver inflammation and fibrosis. *J Clin Invest* 127:55–64.
30. Hoffmann LS, et al. (2015) Stimulation of soluble guanylyl cyclase protects against obesity by recruiting brown adipose tissue. *Nat Commun* 6:7235.
31. Cordero-Herrera I, et al. (2019) AMP-activated protein kinase activation and NADPH oxidase inhibition by inorganic nitrate and nitrite prevent liver steatosis. *Proc Natl Acad Sci USA* 116:217–226.
32. Fujii M, et al. (2013) A murine model for non-alcoholic steatohepatitis showing evidence of association between diabetes and hepatocellular carcinoma. *Med Mol Morphol* 46:141–152.